Formation Wear Resistant Coatings on Martensite Steel Hardox 450 by Welding Methods

S V Konovalov[1]*, V E Kormyshev[1], S A Nevskii[1], Yu F Ivanov[2,3] and V E Gromov[1]

[1]Siberian State Industrial University, Novokuznetsk, 42 Kirov Street, 654007, Russia
[2]Institute of High Current Electronics Siberian Branch of Russian Academy of Science, Tomsk, 2/3 Akademicheskii av., 634034, Russia
[3]National Research Tomsk Polytechnic University, Tomsk, 30 Lenina av., 634050, Russia

*E-mail: konovserg@gmail.com

Abstract. By methods of modern physical materials science the investigations analysis of phase composition, defect substructure, mechanical and tribological properties of Cr-Nb-C-V containing coatings formed in surfacing on martensitic wear resistant steel Hardox 450 were carried out. It was shown that surfacing resulted in the formation of high strength surface layer 6 mm in thinness. This layer had wear resistance 138 times greater than that of the base and friction coefficient 2.5 times less. Having analyzed the deflected mode of the deposited material in conditions of friction, a conclusion is drawn that plastic shear deformation is localized in the surface layer due to the high friction factor, as the result, scratches are formed. The maximum of tangential stress is deflected deep into the material provided that friction factor is low. On the basis of the investigations by methods of X-ray structural analysis and transmission diffraction electron microscopy it was shown that increase strength and tribological properties of surfacing metal were caused by its phase composition and state of defect substructure, namely, availability of interstitial phases (more than 36%) and martensitic type of α-phase structure.

1. Introduction

At present surface and subsurface layers of materials are to meet a lot of requirements because of growing production of high-duty products [1]. These products are used in conditions of enormous loading the surface layers, where most defects are detected. Such processes as wear, corrosion, crack initiation and propagation are the most intense in surface layers; that is the major cause of product performance degradation. Therefore, a surface layer should possess certain characteristics (high hardness and wear resistance, compressive residual stresses etc.). As the consequence, its modification via developing a gradient structure is required [2]. There are some procedures available to synthesize a gradient structure, e.g. electro explosive alloying and electron beam treatment [3], plasma processing [4], various types of weld deposition [5 − 8], laser processing [9]. Weld deposition of wear and corrosion resistant materials is easy-to-implement [7]. This procedure makes it possible to process significant areas of material; that is particularly important for large-dimensional products.

Flux cored wires are applied frequently alongside with electrodes for producing wear resistant deposited layers [10]. However, their wide application is complicated because of insufficient information on the structure, phase composition and hardening mechanisms of the deposited metal in diverse operational conditions. Let us note that the structure and phase composition of material deposited on steel Hardox 400 by electric-arc method have already been studied in our papers [11, 12]. We have found out that secondary phases lead to strengthening, but no detailed consideration of its mechanisms has been provided yet.

Therefore, this paper is focused on the study of synthesizing nanostructural wear resistant coatings and identifying mechanisms of their strengthening.

2. Materials and Methods

Steel Hardox 450 (0.19-0.26 %C, 0.70% Si, 1.60% Mn, 0.25% Cr, 0.25% Ni, 0.25% Mo, 0.004% B, 0.025% P, 0.010% S (Wt. %, ferrum is Bal.))) is used as the base material, weld deposition (1.4 %C, 1.0 %V, 7.0 % Cr, 8.0 % Nb, 1.2 % W(Wt. %, ferrum is Bal.)) is carried out in the shielding gas atmosphere, containing Ar – 98 %, CO_2 – 2 %; welding current is 250–300 A, and welding arc voltage is 30–35 V [11].
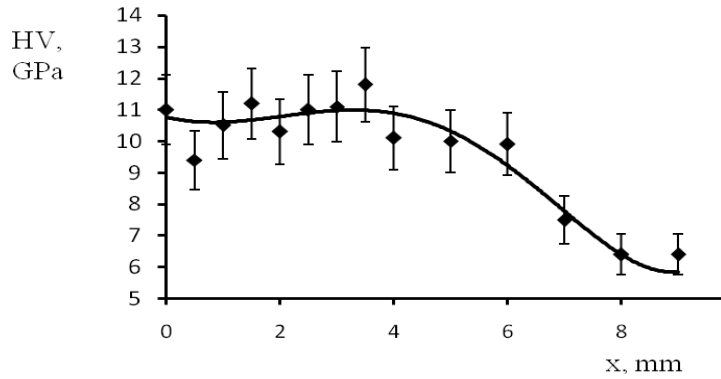
X-ray structural analysis and transmission diffraction electron microscopy are used when studying phase composition and defect substructure of the deposited metal. X-ray structural analysis is carried out by difractometers DRON-7 and Shimadzu XRD 6000 (Bragg-Brentano geometry, cobalt and copper k_α-radiation). To determine phase composition, primary and secondary stresses we rely on methods, outlined in [13]. Microscope EM-125 is used for implementation of transmission electron microscopy analysis. The microstructure is analyzed according to the procedure in [14]. The foils are produced via electrolytic thinning of samples, cut out of the deposited metal, of the deposited metal – steel contact area, and of the steel spaced 15 mm from the area of contact. Mechanical properties of the deposited metal and steel are characterized regarding to microhardness [15] (HVS-1000A). Tribological characteristics of the deposited metal are identified via measuring wear resistance and friction factor (tribotester Tribotechnic). Wear is tested in the following conditions: a ball 3 mm in diameter, made of hard Ti (VK8)-based alloy is used as a counterbody. The counterbody is moved along the circle 4 mm in diameter on the surface of the sample at a linear speed of 2 cm/s and basic load 5 N. The total number of counterbody revolutions is 5000. Wear factor V is calculated as the ratio of the cut out material volume [16] to the sample load and friction length (cross-sectional area of wear groove, as well), and friction factor μ.
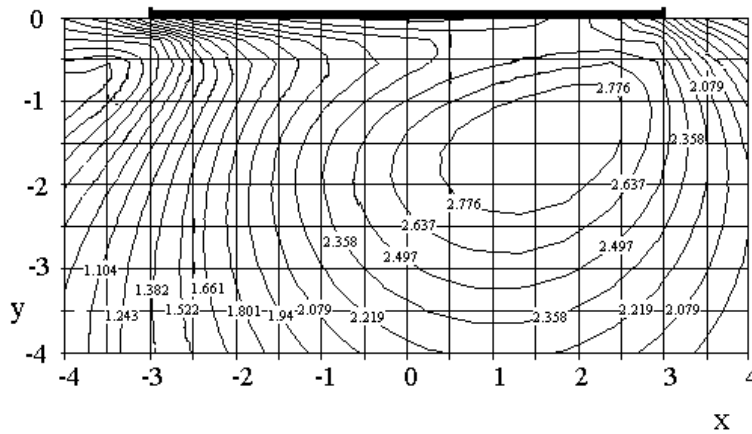
3. Results and discussion

Figure 1 shows the results of microhardness measurement. Analyzing the data, presented in this figure, it should be noted that a high-strength 6 mm thick surface layer is synthesized under weld deposition; and microhardness of this layer varies from 9.5 to 11.5 GPa. Microhardness of the material diminishes fast in a direction away from the deposited metal surface, reaching a level of 6.5 GPa. Therefore, the deposited layer is twice as hard as the base metal, provided that thickness of the deposited layer is ≈6 mm. Wear factor of the deposited layer is $V = 95.1 \cdot 10^{-6}$ mm³/N·m, and that of steel is $V = 0.69 \cdot 10^{-6}$ mm³/N·m as tribological testing the base and deposited metal demonstrates. Friction factors are 0.259 and 0.104 for the deposited metal and base, respectively.

In view of up-to-date physical mesomechanics [17] one should look for an explanation of improving strength properties of the deposited metal on various scale levels of the structure. On a macroscopic level it can be explained due to the changing deflected mode. The approximation below is used to calculate it: normal $\sigma_{yy}(x, y)$ and tangential stresses $\tau_{xy}(x, y)$ are applied to section

$-l \le x \le l$, y = 0   of   an   elastic   semi-plane $-\infty \le x \le \infty$, y ≤ 0;   here $\sigma_{yy}(x,0) = l^2 - x^2$,

$\tau_{xy}(x,0) = \mu \cdot \sigma_{yy}(x,0)$, where μ – friction factor. Kolosov and Muskheshvili method is taken into account to solve the problem [18]. Initiation of plastic flow in conditions of a sliding contact is

detected (provided that yield criterion Tresca [19] is used) relying on the maximal value of the principal tangential stress τ_1. Isolines of stress τ_1 are shown in Figure 2 for $l = 3$, $\mu = 0.3$.

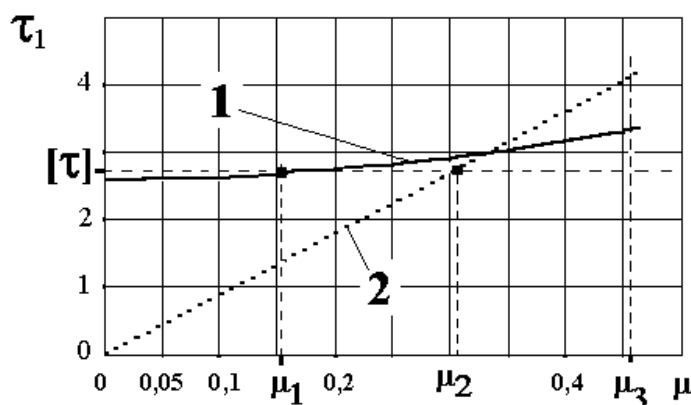**Figure 1.** Microhardness profile of the system «deposited metal / steel»

Figure 2. Isolines of maximal tangential stress for $l = 3$, $\mu = 0.3$, y – depth of sample, x – width of sample

Let us consider the relation of tangential stresses on the surface to maximal tangential stresses in the subsurface layer in dependence of friction factor. The maximal tangential stress in the plane of deformation equals to:

$$\tau_1 = \frac{1}{2}\left(\left(\sigma_{xx} - \sigma_{yy}\right)^2 + 4\tau_{xy}^2\right)^{1/2} \tag{1}$$
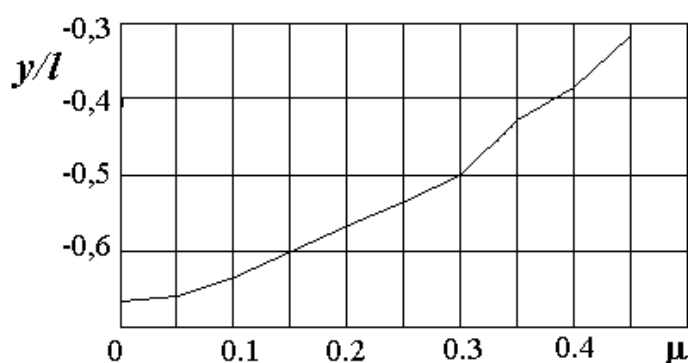
Numerical computations based on formula (1) are provided in [20], their results are presented in Figure 3. Here, $[\tau]$ – stress of shear initiation, τ_1 – maximal tangential stresses, $\tau(x,0)$ – stresses on the surface. As one can see in the Figure, there are no shears anywhere at $\mu < \mu_1$, $\tau_1 < [\tau]$, $\tau(x,0) < [\tau]$, as well as no plastic deformation, leading to material wear, occurs. At $\mu_1 < \mu < \mu_2$, $\tau_1 > [\tau]$, $\tau(x,0) < [\tau]$ tangential stresses exceed the ultimate shear stress in the subsurface layer. At $\mu_2 < \mu < \mu_3$ stresses on the surface and in the layer exceed the ultimate shear stress, that is why, shears are possible both on the surface and in the subsurface layer. At $\mu > \mu_3$ isolation of areas is not registered, and stresses diminish gradually deep into the material. This fact implies that shears occur mainly on the surface; that is illustrated by scratches on the surface.

Their presence can be explained the following way. As soon as plastic shear arises in the subsurface layer, normal and tangential stresses increase on the surface, so scratches occur. The area of maximal tangential stresses is displaced close to the surface, as the result of augmenting friction factor (Figure 4).

Figure 3. Isolines of maximal tangential stress for $l = 3$, $\mu = 0.3$

The growth of the resistance to shear is caused by changing structure and phase states and defect substructure of the material (meso- and micro-scale levels). The results of X-ray phase analysis are given in Table 1. The data in Table 1 show that a deposited metal is a multiphase material. Basic phases (α-phase is not taken into account), relating to interstitial phases, are ferrum oxide, ferrum and chromium carbides. Analyzing the size of coherent scattering areas we can see that dimensions of the phases are in a nanoscale range. Taking into consideration the calculated primary and secondary stresses, a conclusion can be drawn, that ferrum oxide, having a significant strengthening effect together with the matrix, is the cause of the maximal stresses.

Figure 4. The relation of y depth to the length l of section with shear in dependence on friction factor μ

The study on the defect substructure of steel Hardox 450 has revealed that it is a polycrystalline aggregate based on α-phase. In bulk α-phase grains a lamellar structure dominates, being apparently the result of martensite $\gamma \to \alpha$ transformation (Figure 5 a). A sub-grain structure is registered infrequently (Figure 5 b).
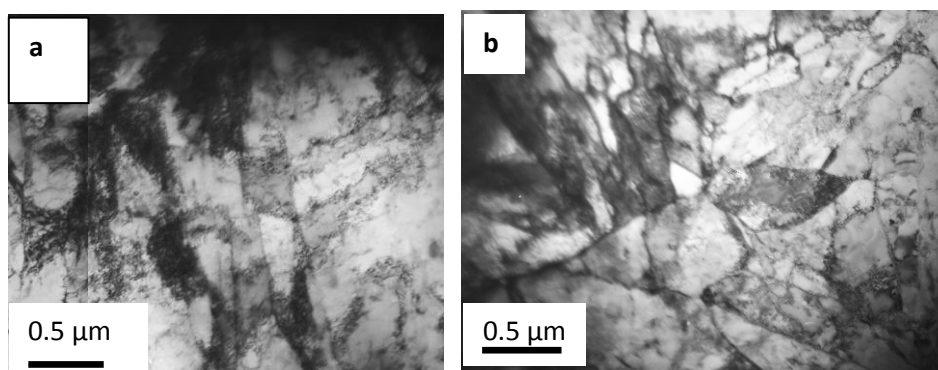
Secondary phase particles are detected in bulk lamellae (Figure 5 b), on boundaries of lamellae and sub-grains (Figure 5 a). We have determined that these particles are ferrum carbide Fe_3C.

The study outcomes of the defect substructure of the deposited material are in line with the data of X-ray phase analysis. The principal phase is α-phase (Figure 6 a). It has a martensite structure. Indexing micro electron diffraction patterns of the martensite structure reveals retained austenite (Figure 6 a (insert) arrows indicate reflexes of retained austenite), which is located on the boundaries of martensite crystals in form of long inter-layers. Figure 6 b and Figure 6 c show images of oxide and carbide phases. Ferrum oxide Fe_3O_4 and vanadium carbide V_8C_7 are detected. It is quite distinct that particles of special carbides are round, dimensions of the particles vary from one to tens nm. Carbide phase particles are located on the boundaries and in bulk martensite crystals.
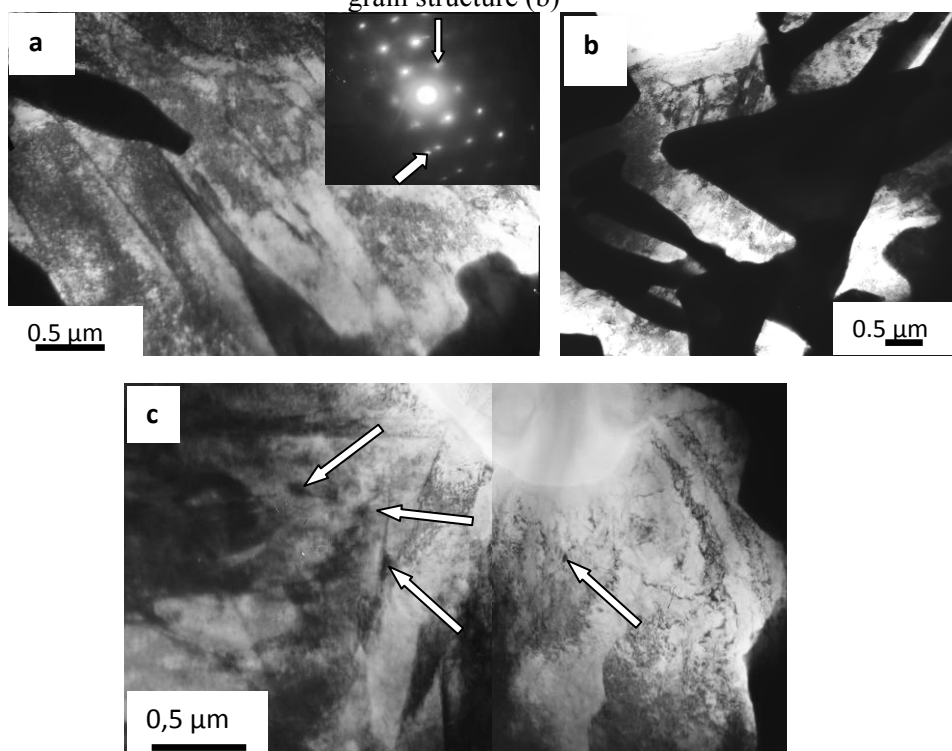
The structure of the deposited - base metal contact area is like the base steel structure in a lot of parameters. The martensite structure is identified. In martensite crystals there is a dislocation substructure in form of chaotically distributed dislocations and dislocation balls.

Table 1. The relation of maximal tangential shear stress τ_1 to friction factor. $[\tau]=2.7$; $\mu_1=0.155$; $\mu_2=0.31$; $\mu_3=0.47$

Phase	Phase characteristics				
	ΔV, mass. %	D (CSR), nm	$\Delta d/d$, 10^{-3}	$\sigma_1+\sigma_2$, MPa	$<\sigma>$, MPa
α-Fe	63.2	24.53	2.03	1413	396
Fe_3O_4	28.8	9.85	7.254	6380	1670
Fe_3C	6.0	14.04	3.395	-	-
CrC	2.0	10.55	2.914	5828	1107

Figure 5. Electron microscope image of steel Hardox 450 structure. Lamellar structure (a), sub-grain structure (b)

Figure 6. Images of the deposited material α-phase (a), ferrum oxide (b), and vanadium carbide (c) structures made by electronic microscopy

4. Conclusion

The structure and properties of material deposited on steel Hardox 450 are studied by methods applied in up-to-date material science on various (macro, micro, and nano) scale levels of the structure. It has been ascertained that microhardness and wear resistance of the deposited layer are twice and 140 folds as high as these characteristics of steel Hardox 450, respectively. Friction factor of the deposited material is four times lower than that of the base. The deflected mode of the material, calculated in conditions of friction, shows that plastic shear deformations are localized in its surface layer. This fact is emphasized by changing surface relief (occurrence of scratches). It has been revealed that mechanical properties of the deposited layer are improved due to formation of multiphase submicro and nanostructures; their strengthening is conditional on the martensite structure of α-matrix and high (more 36 %) inclusion volume fraction of oxide and carbide phases.

Acknowledgements

References

[1]   D'Ans Pierre, Degrez Marc 2015 *Surf. and Coat. Tech.* **276**.
[2]   Yang X, Ma X, Moering J, Zhou H, Wang W, Gong Y, Tao J, Zhu Yu, Zhu X. 2015 *Materials Science and Engineering: A*. **645** 280.
[3]   Sosnin K V , Ivanov Yu F, Gromov V E , Budovskikh E A, D.A. Romanov 2014 *Journal of Surface Investigation. X-ray, Synchrotron and Neutron Techniques.* **8** 1286.
[4]   Béjar̕ M A, Henríquez R 2009 *Materials & Design* **30** 1726.
[5]   Gnyusov S F, Ignatov A A, Durakov V G, Tarasov S Yu 2012 *Applied Surface Science* **263** 215.
[6]   Rao L, Wang Sh, Zhao J, Geng M, Ding G 2014 *Journal of Iron and Steel Research, International* **21** 869.
[7]   Słoma J, Szczygieł I, Sachajdak A 2011 *Archives of Civil and Mechanical Engineering* **11** 437.
[8]   Chen X, Fang Y, Li P, Yu Z, Wu X, Li D 2015 *Materials & Design* **65** 1214.
[9]   Yilbas B S, Shuja S Z 2013 *Laser Surface Processing and Model Studies*, Berlin: Springer.
[10] Senthilkumara B, Kannanb T. 2015 *Measurement* **62** 127.
[11] Kapralov E V, Budovskikh E A, Gromov V E, Ivanov Yu F 2015 *Russian Physics Journal* **58** 471.
[12] Kapralov E V, Raykov S V, Budovskikh E A, Gromov V E, Vashchuk E S and Ivanov Yu.F. 2014 *Bulletin of the Russian Academy of Sciences: Physics* **78** 1015.
[13] Zevin L S, Kimmel G 1995 *Quantitative X-Ray Diffractometry*, Berlin: Springer.
[14] Fultz B, Howe J M 2013 *Transmission Electron Microscopy and Diffractometry of Materials*, Berlin: Springer.
[15] Pelleg J 2013 *Mechanical Properties of Materials*, Berlin: Springer.
[16] Randall N 2002 *CSM Instruments Application Bulletin* **18** 3.
[17] Panin V E, Egorushkin V E, Panin A V 2010 *Physical Mesomechanics* **13** 215.
[18] Muskhelishvili N I 1966 *Nekotorye osnovnye zadachi matematicheskoi teorii uprugosti (Some Basic Problems of Mathematical Elasticity Theory)* Moscow: Nauka.
[19] He Q -C, Vallée C, Lerintiu C 2005 *ZAMP* **56** 357.
[20] Molotkov S G 2006 *Russian Physics Journal* **49** 86.